JOURNAL OF MATERIALS SCIENCE 39 (2004) 6735–6741

Direct measurement of oxygen in lead-based ceramics using the ζ-factor method in an analytical electron microscope

E. P. GORZKOWSKI, M. WATANABE, A. M. SCOTCH, H. M. CHAN, M. P. HARMER
Center for Advanced Materials and Nanotechnology, Lehigh University, Bethlehem, PA 18015, USA
E-mail: epg2@alumni.lehigh.edu

X-ray absorption of oxygen is significant in thin specimens of $Pb(Mg_{1/3}Nb_{2/3})O_3$-35 mol% $PbTiO_3$ [PMN-35PT] due to the presence of heavy elements such as Pb and Nb. Therefore, direct measurement of the oxygen concentration in these types of systems can be difficult. Furthermore, assumption of the composition from stoichiometric considerations may not be feasible, particularly if the valence state of one or more of the cation species is variable. Using only XEDS data, the ζ-factor method provides absorption corrected compositional information. In the present study, it was shown that such data were in very good agreement with the nominal values for PMN-35 PT, whereas the uncorrected data underestimated the oxygen content by 300%. In previous work, it was theorized that the swelling of samples containing excess PbO was linked to changes in the composition of the intergranular liquid phase. The ζ-factor technique was used to show that the oxygen to lead ratio of this second phase changes upon annealing.

1. Introduction

Lead based ceramics such as $PbZr_xTi_{1-x}O_3$ (PZT), $Pb(Mg_{1/3}Nb_{2/3})O_3$ (PMN), and $Pb(Zn_{1/3}Nb_{2/3})O_3$ (PZN), together with their solid solutions with $PbTiO_3$ (PT), are materials which have generated a great deal of interest due to their outstanding piezoelectric properties. To date, for PMN:PT and PZN:PT, key parameters such as the longitudinal coupling coefficient (k_{33}), or the effective piezoelectric coefficient (d_{33}), have been maximized for single crystals with compositions near the morphotropic phase boundary (MPB) [1, 2]. The incorporation of the aforementioned single crystal materials into existing devices holds the promise for more precise actuators [3], more powerful undersea transmitters for sonar applications (i.e., surveillance, tactical, navigation) [4], and more sensitive ultrasonic transducers for medical imaging applications [5, 6].

Conventionally, single-crystals of these ceramics are formed by melt techniques such as high temperature solution growth from PbO-based fluxes [7] and modified Bridgman growth [8]. These methods are suitable for growing bulk single crystals, but have relatively slow growth rates and are not readily transferable to large-scale manufacturing. The seeded polycrystal conversion (SPC) process [9] is an alternative single-crystal growth method that offers some advantages over the melt techniques. This process entails bonding a seed single crystal to a polycrystalline precursor of the same composition, and annealing to promote migration of the single-crystal boundary through the polycrystal, hence resulting in a large single crystal. This method is potentially more cost-effective, able to provide for niche applications (such as 1-3 piezo-composites [4]), and directly compatible with current manufacturing of polycrystalline components.

The SPC process has been proven feasible in growing single crystals of $Pb(Mg_{1/3}Nb_{2/3})O_3$-35 mol% $PbTiO_3$ (PMN-35PT) [10, 11], a composition near the MPB. In addition, growth of these single crystals has been shown to be critically dependent on a grain boundary wetting PbO-based liquid second phase within the polycrystalline PMN-35PT precursor [11]. However, recent experiments have demonstrated that the presence of the PbO-based liquid phase is linked to a swelling phenomenon, whereby the density decreases significantly (from 8.1 g/cm^3 to ~7.6 g/cm^3) when air hot-pressed samples are further annealed in air [12]. The observation that the density stays constant when PMN:PT samples are sintered and annealed in oxygen [13] suggests the strong possibility that oxygen is playing a role. In an effort to further understand the swelling issue, it was decided to determine the oxygen content of the intergranular second phase using AEM (analytical electron microscopy).

The quantitative analysis of a material such as PMN-35PT, which contains significant amounts of high atomic number elements such as Pb and Nb, presents several challenges. For example, the use of Electron Energy-Loss Spectrometry (EELS) is not suitable, because for the standard range of energy loss (<2 keV),

the quantification of heavy elements is restricted to the energy-loss edges of M or N shells, where the cross-section models have not been well established. The presence of such heavy elements also limits XEDS (X-ray Energy Dispersive Spectrometry) quantification because X-rays from light elements such as O and Mg are significantly absorbed, even in thin foil specimens. As a result, the weight fractions of light elements may be severely underestimated. Given that the purpose of the present study was to examine the oxygen content, and that Pb can exhibit different valence states, the practice of assuming the oxygen content based on stoichiometric considerations is clearly not feasible.

The conventional method for correcting for X-ray absorption requires determination of the specimen thickness at every point in the specimen from which spectra are acquired. Clearly, this procedure can be both time consuming and contribute additional sources of experimental error. The advantage of the ζ-factor approach is that once the value of the ζ-factor has been determined for the given operating conditions, it can be used to simultaneously evaluate the specimen thickness and absorption corrected compositional data. A brief summary of the technique is provided in Section 3.1. For more details, the reader is referred to references 14 and 15. This paper describes the application of this approach to the compositional analysis of the intergranular PbO-based phase. The implications of the results to swelling will be discussed.

2. Experimental procedure

PMN-35PT powder (TRS Ceramics) was divided into two batches. One of the batches was modified by the addition of 5 vol% of excess PbO (Alfa Aesar 99.9995%). The powders were ball-milled in ethanol for 24 h using zirconia milling media, and subsequently dried and calcined at 450°C for 4 h in air. Next the powders were ground using an agate mortar and pestle, and passed through a 100-mesh sieve. Pressed pellets (nominally 13 mm in diameter) were fabricated by uniaxial pressing at 10 MPa in an Al_2O_3 die, followed by cold isostatic pressing at 340 MPa. Subsequently, the pellets were hot-pressed (in air) at 20 MPa for 30 min at 880°C to produce fully dense samples. After hot pressing, each disk was sectioned into six pieces. Specimens were annealed at 1150°C for times ranging from 0–5 h, then quenched. The annealing treatments were carried out using a double crucible arrangement, with the samples embedded in packing powder to avoid PbO volatilization [12].

Thin foil specimens for AEM characterization were prepared in the following manner. First, the samples were mounted in epoxy resin and polished down to 0.05 μm SiO_2. The samples were subsequently removed from the epoxy, and coated with gold-palladium for thin specimen preparation using an FEI Strata DB235 dual beam focused ion beam (FIB) system. In the present study, the use of the FIB was very advantageous, in that specific boundaries could be selected and extracted for analysis. The final thickness of the FIB thin sections was less than 200 nm after sample preparation using the lift-out technique. An example of one of these samples can be seen in Fig. 2; this scanning electron image was taken just after final ion thinning and demonstrates the versatility of the dual beam FIB over the single beam system. The thin sections were removed with an electrostatic glass-rod plucking device and placed on a Cu grid coated with carbon for AEM examination.

TABLE I Comparison of ICP-OES data for PMN-35PT standard to the theoretical PMN-35PT values in weight fraction (NB: For ICP PB and O are determined by difference)

	Nominal values (wt%)	ICP-OES results (wt%)
Mg	1.66	1.66
Nb	12.68	12.63
Pb	65.26	65.31
O	15.12	15.14
Ti	5.28	5.26
Total	100	100

A hot-pressed and annealed sample with 0% excess PbO was sent for ICP-OES (Inductively Coupled Plasma Optical Emission Spectroscopy) wet chemical analysis to verify the composition. The results, which were found to agree closely with the nominal values, are shown in Table I. Quantitative chemical analysis was performed on a VG HB603 AEM operating at 300 kV. Elemental maps were obtained for each element using an Oxford/Link windowless Si(Li) XEDS detector attached to the AEM. The beam current was measured before and after a series of measurements using a Faraday cup and found to be approximately 0.5 nA. In this study, since values of the Cliff-Lorimer k-factors and the ζ-factor must be determined by using at least one thin specimen with known composition, the 0% excess PbO sample was used as a standard.

3. Results and discussion

3.1. Brief description of ζ-factor method

For quantification of thin-foil specimens in the AEM, the Cliff-Lorimer ratio technique [16] is generally applied. The compositions of constituent elements (C_A and C_B, usually defined as the weight fraction) in a thin specimen can be determined from the measured characteristic X-ray intensities corresponding to the elements (I_A, I_B) as:

$$\frac{C_A}{C_B} = k_{AB}\frac{I_A}{I_B} \tag{1}$$

where k_{AB} is the Cliff-Lorimer factor, the value of which can be determined both theoretically and experimentally [17]. In order to account for X-ray absorption, Goldstein *et al.* have modified the Cliff-Lorimer ratio equation as follows [18]:

$$\frac{C_B}{C_A} = k_{AB}\left(\frac{I_B}{I_A}\right)\left[\frac{(\mu/\rho)^A_{sp}}{(\mu/\rho)^B_{sp}}\right] \times \left\{\frac{1-\exp\left[-(\mu/\rho)^B_{sp}\rho t\ \mathrm{cosec}(\alpha)\right]}{1-\exp\left[-(\mu/\rho)^A_{sp}\rho t\ \mathrm{cosec}(\alpha)\right]}\right\} \tag{2}$$

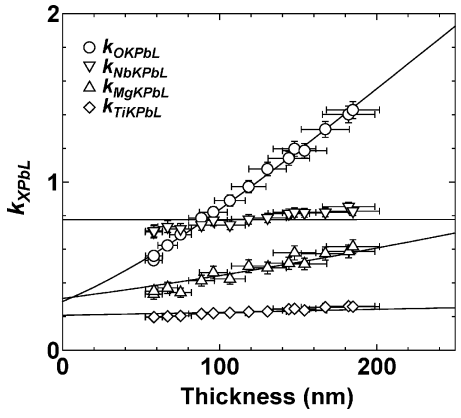

Figure 1 k-factor vs. thickness data that is used in order to calculate ζ factor and absorption free k-factors used in the calculations in Table I. (The k_{NbPb} fits very well for the range of thickness that was used in the study.)

where $(\mu/\rho)^{\mathrm{A}}_{\mathrm{sp}}$ and $(\mu/\rho)^{\mathrm{B}}_{\mathrm{sp}}$ are the mass absorption coefficients of the characteristic X-ray lines, ρt is the mass thickness (ρ: density, t: specimen thickness) and α is the X-ray take-off angle. As can be seen from the above equation, application of the absorption correction requires knowledge of the specimen density and thickness at each point of analysis. As mentioned earlier, this is a major limitation because such measurements are tedious, and more importantly can give rise to further errors in the quantification.

The ζ-factor method was proposed in order to overcome these limitations and difficulties [14]. In a thin-foil specimen, it can be assumed that the characteristic X-ray intensity is proportional to the mass thickness, ρt, providing X-ray absorption and fluorescence are negligible. We can therefore write:

$$\rho t = \zeta_{\mathrm{A}} \frac{I_{\mathrm{A}}}{C_{\mathrm{A}}} \tag{3}$$

where the ζ factor (ζ_{A}) is the factor relating I_{A} to ρt and C_{A}. By substituting Equation 3 into Equation 2, the mass thickness term can be eliminated:

$$\frac{C_{\mathrm{B}}}{C_{\mathrm{A}}} = k_{\mathrm{AB}} \left(\frac{I_{\mathrm{B}}}{I_{\mathrm{A}}} \right) \left[\frac{(\mu/\rho)^{\mathrm{A}}_{\mathrm{sp}}}{(\mu/\rho)^{\mathrm{B}}_{\mathrm{sp}}} \right] \times \left\{ \frac{1 - \exp\left[-(\mu/\rho)^{\mathrm{B}}_{\mathrm{sp}} \zeta_{\mathrm{A}} (I_{\mathrm{A}}/C_{\mathrm{A}}) \operatorname{cosec}(\alpha) \right]}{1 - \exp\left[-(\mu/\rho)^{\mathrm{A}}_{\mathrm{sp}} \zeta_{\mathrm{A}} (I_{\mathrm{A}}/C_{\mathrm{A}}) \operatorname{cosec}(\alpha) \right]} \right\} \tag{4}$$

Using the above equation, absorption-corrected compositions can be determined once the k and ζ factors are known [14].

3.2. Determination of k and ζ-factors

To determine the k and ζ-factors the same limitation exists as for the original Cliff-Lorimer ratio method; namely, at least one standard thin specimen with known composition is required. In this study, PMN-35PT with 0% PbO was used as the standard since the specimen contains all of the elements of interest. In the case of the Pb-L_α line, because the degree of absorption is below 3% up to a specimen thickness of 300 nm, the intensity will scale linearly with the thickness. However, as should be apparent from comparing Equations 1 and 4, for elements for which there is significant absorption, the correction term gives rise to an *apparent* k-factor. Within the apparent k-factor, there are two terms which are unknown; namely, the 'true' k-factor (or absorption free k-factor), and the ζ-factor. By measuring a series of X-ray intensity ratios over a range of thickness values, it is possible to determine both these quantities by a non-linear least squares fitting. Once the value of the

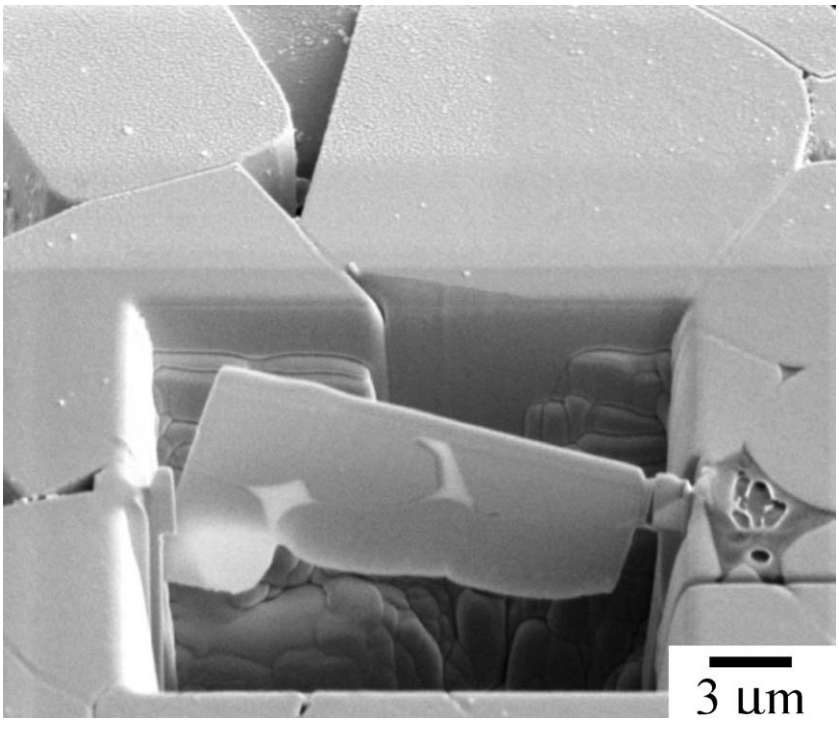

Figure 2 Secondary electron image of a TEM sample prepared using a dual-beam FIB. (Note the bright areas are indications of electron transmission in SEM mode.)

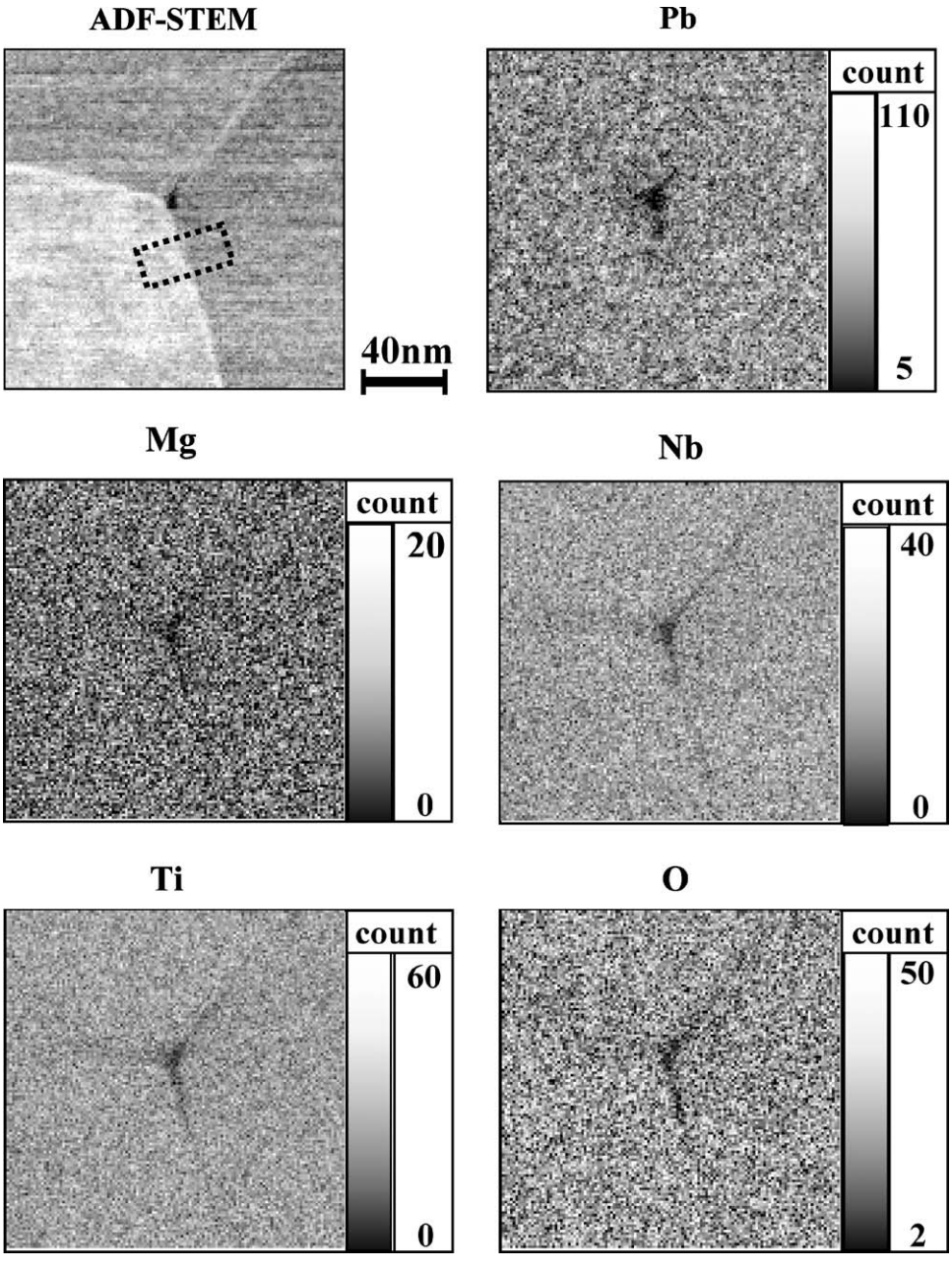

Figure 3 (a) Annular dark field image of triple point. X-ray map of weight fraction, (b) lead, (c) niobium, (d) magnesium, (e) titanium, and (f) oxygen.

ζ-factor is known, thickness values can be calculated using Equation 3. Note that for the specimen density (ρ) of the 0% excess PbO PMN-35PT sample, a measured value of 8.1 g/cm^3 was used.

Fig. 1 shows the measured k values of the O-K$_\alpha$, Mg-K$_\alpha$, Ti-K$_\alpha$ lines with respect to the Pb-L$_\alpha$ intensity, plotted against the specimen thickness. (The error bars represent a 99% confidence level (3σ)). The solid lines in Fig. 1 indicate the results of non-linear least squares fitting and are well superimposed on the measured k values. The absorption free k-factors can be obtained from the extrapolated k-values at zero thickness.

3.3. Validation of quantification by the ζ-factor method

In the case of the PMN-35 PT standard, the experimentally determined composition data were compared with the nominal values (see Table II). Both the uncorrected data, and the values obtained after correcting for absorption are included. Note that the composition of the standard was independently confirmed by ICP-OES wet chemical analysis. The quoted uncertainty level for the experimental results represent the 99% confidence level (3σ). It is clear that the application of the absorption correction has a significant influence

TABLE II Comparison of corrected and uncorrected composition data in weight percent from a PMN-35PT standard to theoretical PMN-35PT values

	Measured (corrected)	Measured (uncorrected)	Theoretical
Mg	1.6 ± 0.2	1.2 ± 0.3	1.66
Nb	12.7 ± 0.5	12.7 ± 1.4	12.68
Pb	65.4 ± 1.1	75.6 ± 3.9	65.26
O	15.1 ± 0.4	5.5 ± 1.9	15.12
Ti	5.3 ± 0.3	4.9 ± 0.7	5.28
Total	100.1	99.9	100

on the data. In particular, it can be seen that for the non-corrected case, the oxygen content was underestimated by 300%. The corrected result, however, was in very good agreement with the nominal value. This method of analysis is clearly advantageous as it allows for the direct measurement of oxygen concentration, as opposed to assuming values based on considerations of stoichiometry.

3.4. Quantitative X-ray mapping

As described previously, the dual beam FIB system was used exclusively for thin-specimen preparation for transmission electron microscopy (TEM) and X-ray compositional mapping in the STEM. Fig. 3a depicts an annular dark field STEM image, and 3b–f represent X-ray intensity maps of the (b) Pb-L_α, (c) Mg-K_α, (d) Nb-K_α , (e) Ti-K_α, and (f) O-K_α lines, respectively. These X-ray maps were recorded with 128 × 128 pixels for a dwell time of 200 ms at a single pixel. For the maps, the net intensity was determined by subtracting the background intensities from the peak-intensities. It can be seen that these maps reveal lower intensity regions at the triple point and along the boundaries in all the elemental maps. However, it is known that both compositional and thickness differences can lead to such variations in the X-ray intensity.

In order to determine true compositional maps, the ζ-factor method quantification procedure was applied to the intensity maps. Fig. 4 shows the corresponding mass thickness map (a) and composition maps of (b) Pb, (c) Mg, (d) Nb, (e) Ti, and (f) O. As mentioned above, if the specimen density is known locally, the specimen thickness map can be extracted. In

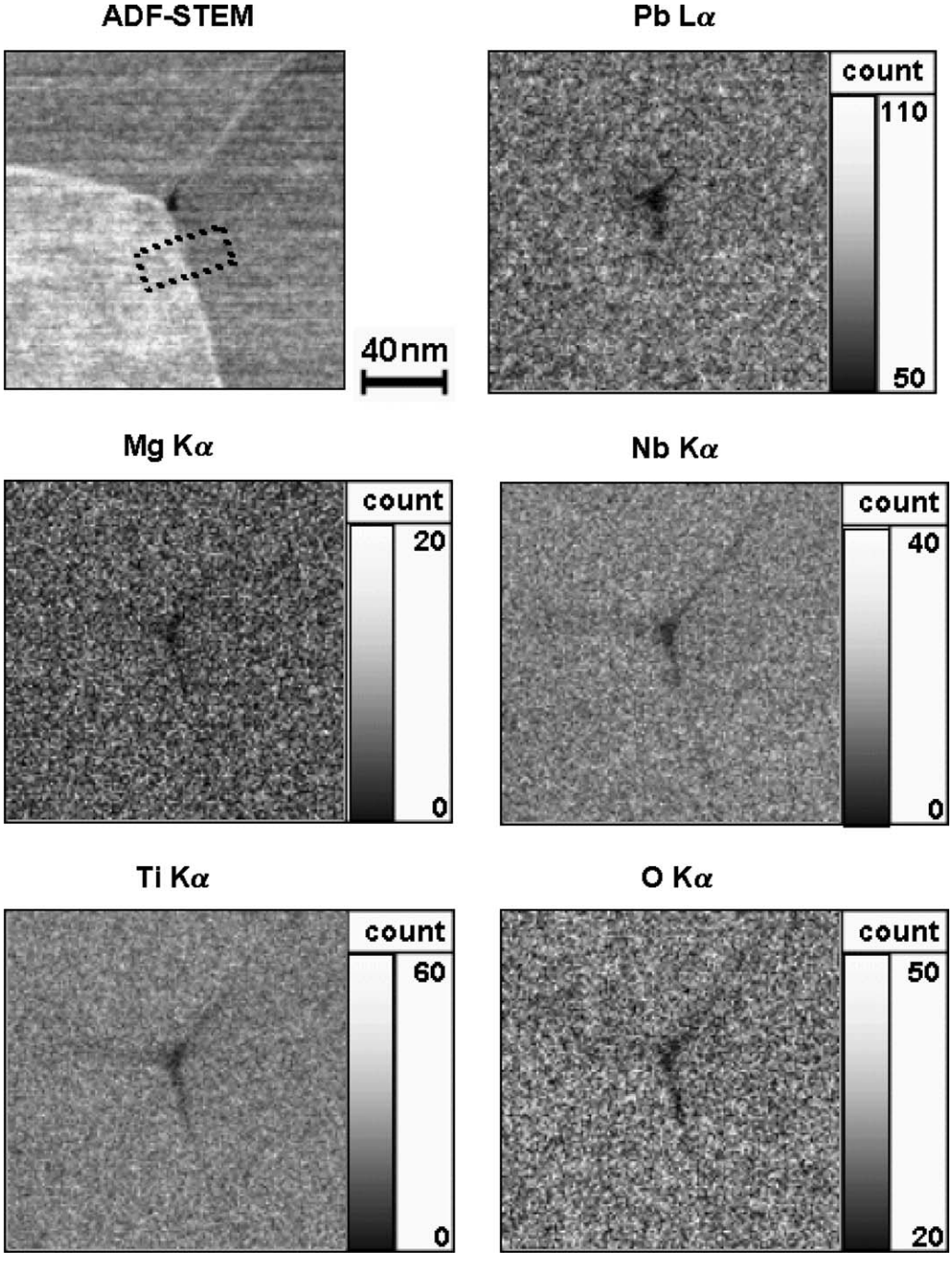

Figure 4 (a) mass thickness map and composition maps of, (b) Pb, (c) Mg, (d) Nb, (e) Ti, and (f) O quantified by the ζ-factor method.

comparison with the intensity maps shown in Fig. 3, the contrast differences between the bulk region and the boundaries are less pronounced. Further, the corrected composition maps of Mg, Nb, Ti, and O show minor depletion around the triple point. Conversely, the Pb composition map shows enrichment at the boundaries; a result which is in marked contrast to that shown by the Pb-L_α net intensity map (Fig. 3b). This latter result illustrates the importance of quantification and the gathering of elemental maps from all the constituents in the system.

As demonstrated above, it can be misleading to evaluate local elemental distributions only using intensity maps of selected elements, which may be a typical approach by XEDS and/or EELS in AEM. The appropriate quantification should eliminate any contributions from local thickness variation and provide true composition distributions even in the thin specimen. The practice of absorption correction should always be followed in these lead based ceramic systems.

3.5. Variation of O/Pb ratio

Once the elemental maps have been collected for each sample, it is a relatively simple process to extract compositional data from line scans across grain boundaries. Fig. 5 shows one such compositional profile, which was obtained from the marked area in Fig. 3a. It should also be mentioned that for the line scans, the result is taken as the addition of 20 lines because of the improvement in counting statistics. Note that the results of both the line scan and the composition map show that the lead content in the boundary is higher than in the grain. This result is not unexpected, given that the intergranular phase has the nominal composition of PbO, which is 88 weight percent Pb, whereas the matrix grains should consist of ∼65 wt% Pb.

Interestingly, the line scan data revealed a difference in the ratio of oxygen to lead between the as hot-pressed and annealed samples. Hence the O/Pb (atomic) ratio was found to be 1.59 in the as hot-pressed sample, whereas all the annealed samples exhibited an O/Pb ratio of 1. This result clearly points to the presence of higher oxides of lead in the as hot-pressed condition. The work of White and Roy [19] and later Risold [20] summarized the transformations that PbO encounters starting at ∼200°C. A summary of their findings is as follows:

$$PbO_2(tetr) \overset{293^\circ C}{\rightarrow} Pb_{12}O_{19} \overset{\sim 300^\circ C}{\Leftrightarrow} Pb_{12}O_{17} \overset{\sim 350^\circ C}{\Leftrightarrow} Pb_3O_4 \overset{\sim 535^\circ C}{\Leftrightarrow} PbO(ortho) \quad (5)$$

It was also shown that pressure can have a large effect on these transformations. For example phases such as Pb_2O_3 and $Pb_{12}O_{19}$ (where the ratio of oxygen to lead is 1.5 and 1.58 respectively), can be formed by applying ∼16,000 psi (110 MPa) at 600°C. It seems plausible, therefore, that upon hot-pressing in the presence of oxygen the excess PbO transforms to one of the higher order lead oxides, thus accounting for the higher oxygen content. It is postulated that when the sample is subsequently annealed at 1150°C, the excess oxygen is given off and causes porosity to develop. A more detailed description of the swelling phenomenon is described elsewhere [21]. The results of the present work highlight the value of the ζ-factor method. Only by direct measurement of the oxygen concentration was it possible to identify the presence of higher order lead oxides, and hence rationalize the swelling effect. Clearly this type of approach has great general utility for the characterization of light elements in ceramics.

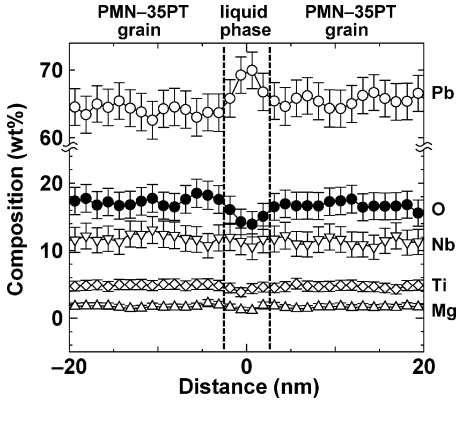

Figure 5 Compositional profile across the interface extracted from the maps shown in Fig. 3.

4. Summary

The ζ-factor approach works very well for lead-based ceramics and provides a viable method to directly measure the oxygen concentration. It was shown that the corrected data fit very well to the theoretical values for PMN-35 PT, while the uncorrected data underestimated the oxygen content by 300%. Additionally, it was found that the oxygen to lead (atomic) ratio changes from 1.59 (in the as hot-pressed state) to ∼1 (after annealing). This result is attributed to the formation of higher order lead oxides ($Pb_{12}O_{19}$, Pb_2O_3) during processing, which transform to PbO during annealing. The evolution of the excess oxygen is believed to be the cause of the observed swelling in these samples.

Acknowledgments

The authors wish to thank Dave Ackland for his help using the VG HB603 and FEI Strata 235DB. The author (MW) wishes to acknowledge Bechtel Bettis Laboratories and NSF DMR-0304738, while the author (EPG) wishes to thank AFOSR, under Grant No. F49620-99-1-0340, DARPA/ONR under Contract No. N00014-96-I-0627 and PA Dept of Community and Economic Development under contract 20-906-0009 for support.

References

1. S.-E. PARK and T. R. SHROUT, *IEEE Trans. Ultrasonics, Ferroelectr. Frequency Contr.* **44**(5) (1997) 1140.
2. *Idem., J. Appl. Phys.* **82**(4) (1997) 1804.
3. *Idem., Mater. Res. Innovat.* **1** (1997) 20.
4. K. McNEAL, C. NEAR, R. GENTILMAN, M. HARMER, H. CHAN, A. SCOTCH, V. VENKATARAMAN and C. GRESKOVICH, *Proceedings of SPIE* **3675** (1999) 330.

5. S. SAITOH, M. IZUMI, S. SHIMANUKI, S. HASHIMOTO and Y. YAMASHITA, U.S. Patent 5,295,487, 1994.
6. P. D. LOPATH, S.-E. PARK, K. K. SHUNG and T. R. SHROUT, *Proceedings of the IEEE Ultrasonics Symposium* **2** (1997) 1643.
7. T. R. SHROUT, Z. P. CHANG, N. KIM and S. MARKGRAF, *Ferroelectric Lett.* **12** (1990) 63.
8. K. HARADA, S. SHIMANUKI, T. KOBAYASHI, S. SAITOH and Y. YAMASHITA, *J. Amer. Ceram. Soc.* **81**(11) (1998) 2785.
9. M. P. HARMER, H. M. CHAN, H.-Y. LEE, A. M. SCOTCH, T. LI, F. MESCHKE and A. KHAN, US Patent #6,048,394, 2000.
10. T. LI, A. M. SCOTCH, H. M. CHAN, M. P. HARMER, S.-E. PARK, T. R. SHROUT and J. R. MICHAEL, *J. Amer. Ceram. Soc.* **81**(2) (1998) 244.
11. A. KHAN, F. A. MESCHKE, T. LI, A. M. SCOTCH, H. M. CHAN and M. P. HARMER, *ibid.* **82**(12) (1999) 2958.
12. A. KHAN, E. P. GORZKOWSKI, A. M. SCOTCH, H. M. CHAN and M. P. HARMER, *ibid.* **86**(12) (2003) 2176.
13. A. M. SCOTCH, H. M. CHAN and M. P. HARMER, submitted to *J. Am. Ceram. Soc.* (2003).
14. M. WATANABE, Z. HORITA and M. NEMOTO, *Ultramicroscopy* **65**(3/4) (1996) 187.
15. G. LUCADAMO, M. WATANABE, K. BARMAK, D. B. WILLIAMS, C. MICHAELSEN and R. ALANI, *Philosoph. Mag.* A **79**(6) (1999) 1423.
16. G. CLIFF and G. W. LORIMER, *J. Microscopy* **103** (1975) 203.
17. D. B. WILLIAMS and C. BARRY CARTER, "Transmission Electron Microscopy" (Plenum Press, NY, 1996).
18. J. I. GOLDSTEIN, J. L. COSTLY, G. W. LORIMER and S. J. B. REED, in "SEM 1977," Vol. 1, edited by O. Johari (IITRI, Chicago, IL, 1977) p. 315.
19. W. B. WHITE and R. ROY, *J. Amer. Ceram. Soc.* **47**(5) (1964) 242.
20. D. RISOLD, J.-I. NAGATA and R. O. SUZUKI, *J. Phase Equilibria* **19**(3) (1998) 213.
21. A. M. SCOTCH, E. P. GORZKOWSKI, H. M. CHAN and M. P. HARMER, submitted to *J. Amer. Ceram. Soc.* (2/2004).

Received 11 December 2003
and accepted 20 January 2004